

X-ray polarization spectroscopy to study anisotropic velocity distribution of hot electrons produced by an ultra-high-intensity laser

Y. Inubushi,^{1,2,*} Y. Okano,¹ H. Nishimura,¹ H. Cai,¹ H. Nagatomo,¹ T. Kai,¹ T. Kawamura,³ D. Batani,⁴ A. Morace,⁴ R. Redaelli,⁴ C. Fourment,⁵ J. J. Santos,⁵ G. Malka,⁵ A. Boscheron,⁶ O. Bonville,⁶ J. Grenier,⁶ Ph. Canal,⁶ B. Lacoste,⁶ C. Lepage,⁶ L. Marmande,⁶ E. Mazataud,⁶ A. Casner,⁷ M. Koenig,⁸ S. Fujioka,¹ T. Nakamura,¹ T. Johzaki,¹ and K. Mima¹

¹*Institute of Laser Engineering, Osaka University, Suita, Osaka, Japan*

²*Graduate School of Engineering, Osaka University, Suita, Osaka, Japan*

³*Tokyo Institute of Technology, Yokohama, Kanagawa, Japan*

⁴*Dipartimento di Fisica "G. Occhialini," University of Milano-Bicocca, Milan, Italy*

⁵*CELIA, Université de Bordeaux/CNRS/CEA, Talence, France*

⁶*CEA/CESTA, Le Barp, France*

⁷*CEA-DAM, DIF, F-91297 Arpajon, France*

⁸*LULI, Ecole Polytechnique, Palaiseau Cedex, France*

(Received 14 February 2009; revised manuscript received 2 March 2010; published 24 March 2010)

The anisotropy of the hot-electron velocity distribution in ultra-high-intensity laser produced plasma was studied with x-ray polarization spectroscopy using multilayer planar targets including x-ray emission tracer in the middle layer. This measurement serves as a diagnostic for hot-electron transport from the laser-plasma interaction region to the overdense region where drastic changes in the isotropy of the electron velocity distribution are observed. These polarization degrees are consistent with analysis of a three-dimensional polarization spectroscopy model coupled with particle-in-cell simulations. Electron velocity distribution in the underdense region is affected by the electric field of the laser and that in the overdense region becomes wider with increase in the tracer depth. A full-angular spread in the overdense region of $22.4^{+5.4}_{-2.4}$ was obtained from the measured polarization degree.

DOI: [10.1103/PhysRevE.81.036410](https://doi.org/10.1103/PhysRevE.81.036410)

PACS number(s): 52.70.La, 52.38.Ph

I. INTRODUCTION

Energy transport by hot electrons in ultra-high-intensity laser produced plasmas is important to deal with high-energy density physics such as fast ignition [1,2] and short pulse x-ray generations [3]. There are two major components of electrons in such plasmas. One is hot electrons, which transfer absorbed laser energy to deeper and higher density plasma regions. Hot electrons are predominantly generated by collective processes in the laser-plasma interaction region [4]. Therefore, their velocity distribution function (VDF) is significantly affected by the electromagnetic field of the incident laser and by the electrostatic field in the plasma. The hot-electron VDF becomes highly anisotropic. The other, background bulk electrons form a return current as a counter stream to the hot electrons and gain energy mostly via Ohmic heating and/or collisional processes [5–7]. Thus, bulk electrons have a thermal distribution and their VDF is largely isotropic. Measurement of anisotropy of hot-electron VDF inside plasma is critical for clarifying energy transport in ultra-high-intensity laser produced plasmas [8]. In particular, such transport is important for fast ignition; the transport of hot electrons from the region where they are produced to the dense fuel accomplishes target ignition. In addition, the anisotropy of the VDF is a key in determining the divergence of the hot-electron beam in the target [9,10]. The anisotropy of the VDF is a crucial parameter in determining the onset of

the Weibel instability which may be an important factor in hot-electron transport inside the target [11].

Polarization spectroscopy is a useful diagnostic tool for measuring the anisotropy of the electron VDF inside plasma. This has been used both in the visible and in the x-ray spectral domains and applied to study both astrophysical [12,13] and laboratory plasmas [14–16]. In general, polarized x rays are emitted because of alignment caused by distortions in the electron VDF [14]. The anisotropy of the electron VDF is evaluated from the polarization degree P of the emitted x rays

$$P = \frac{I_{\parallel} - I_{\perp}}{I_{\parallel} + I_{\perp}}. \quad (1)$$

Here, I_{\parallel} and I_{\perp} are the spectrally integrated intensities of the x-ray emission with electric fields parallel and perpendicular to the electron-beam propagation axis, respectively. The overall polarization degree depends on both the shape of the VDF and its average energy [15,16].

Studies of the electron VDF using x-ray polarization spectroscopy have been performed at relatively low-temperature (a few hundred eV) corona plasma produced by a tabletop repetition laser system having an intensity of 10^{17} W/cm² [16–18]. The present paper reports an experiment using a single-shot, high-power laser and a triple-layer planar target including a chlorinated plastic tracer layer. The dependence of the polarization degrees of Cl-He α line on the position of the tracer layer distributing in an expanding plasma was measured to determine variation of anisotropy of electron

*yinubusi@eie.eng.osaka-u.ac.jp

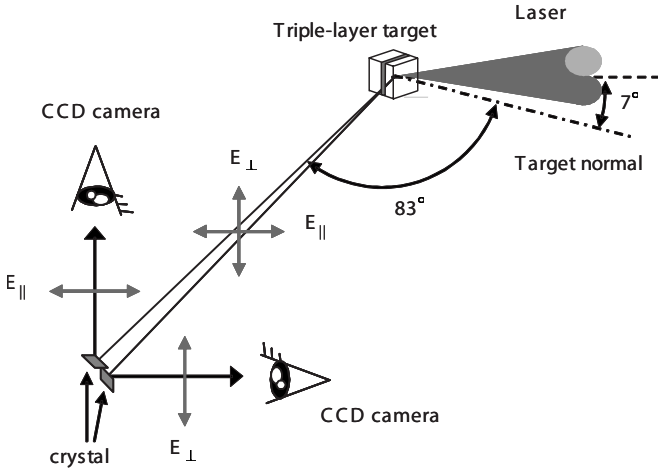


FIG. 1. Experimental setup. Two polarized components of the Cl-He α line emitted from a tracer layer of the triple-layer target were simultaneously observed using a two-channel x-ray spectrometer. Here, E_{\parallel} is the parallel electric field relative to the electron-beam propagation axis while E_{\perp} is the perpendicular component.

VDF. These experimental results are compared to theoretical model of a three-dimensional (3D) polarization spectroscopy model [17] coupled with particle-in-cell simulations.

II. EXPERIMENTAL SETUP

The experiment was carried out using the Alisé laser system at CEA/CESTA in Bordeaux. The system provided a 1.053 μm laser pulse of ~ 10 J energy with ~ 1 ps duration. The *s*-polarized pulse was focused using an $f/3$ off-axis parabolic mirror. The experiment was performed at two different laser intensities by changing the laser spot size, 5×10^{17} W/cm 2 (“low intensity”) and 4×10^{18} W/cm 2 (“high intensity”). A pedestal component arrives prior to the main pulse and grows from the undetectable level to 10^{-6} of the laser peak intensity in 6 ns duration. The targets were triple-layer planar targets consisting of a $2 \times 2 \times 2$ mm 3 polyethylene substrate, a 0.5- or 0.6- μm -thick C $_2$ H $_2$ Cl $_2$ tracer layer, and a parylene (C $_8$ H $_8$) overcoat layer. The thickness of the overcoat layer was varied from 0 to 5 μm in order to change the location of the tracer layer. Two polarized components of the Cl-He α line were simultaneously measured using a two-channel x-ray polarization spectrometer. The spectrometer consists of two identical toroidally curved crystal spectrometers whose dispersion planes are oriented perpendicularly to each other. Two α -quartz crystals were used in (10-11) reflection and positioned 1162 mm away from the plasma. Two charge coupled device (CCD) detectors were used as spectrum recorders. The Cl-He α line was observed at the Bragg angle of 41.7 $^\circ$, close enough to 45 $^\circ$ to ensure that the crystals work as a polarizer. Inclusion of orthogonal polarization components were corrected assuming Bragg reflection for a perfect crystal. Relative sensitivities of the two channels had been cross-calibrated beforehand on Alisé laser system with accuracy of $\pm 3.4\%$ by adjusting the two spectrometers so that they receive the same signal. Figure 1 shows the experimental setup. The incident

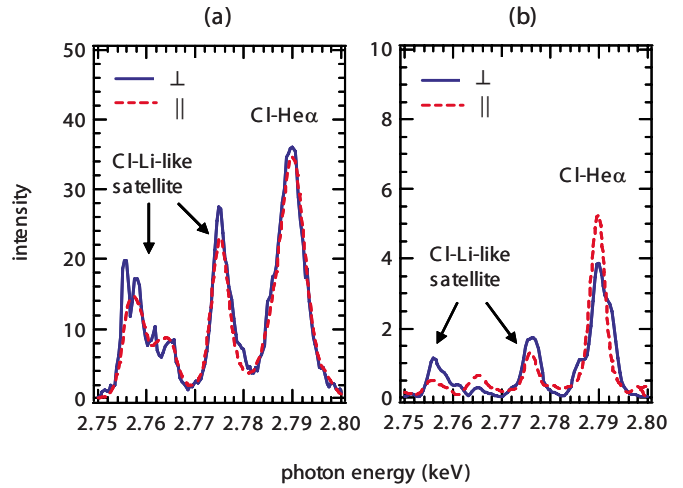


FIG. 2. (Color online) X-ray spectra measured for a tracer depth of (a) 0.1 μm and (b) 2.1 μm in the low-intensity case (5×10^{17} W/cm 2). \perp and \parallel mean the perpendicular component of the x-ray emission and the parallel component, respectively. Polarization degrees of (a) -0.06 and (b) 0.10 were obtained from the spectrally integrated intensities of the Cl-He α line.

angles of the laser pulse on the target and the line-of-sight angle of the spectrometer were 7 $^\circ$ and 83 $^\circ$ with respect to the target normal, respectively. The dispersion plane of one crystal was set parallel to the laser axis to detect the perpendicular component of the Cl-He α line, while the other was set perpendicular to detect the parallel component.

III. EXPERIMENTAL RESULTS AND DISCUSSION

Figure 2 shows x-ray spectra measured for tracer depths of (a) 0.1 μm and (b) 2.1 μm in the low-intensity case. The tracer depth is hereafter defined as the thickness of the parylene overcoat layer. Both Cl-He α line and Li-like satellite lines were observed for all cases. It is shown in Fig. 2(a) that the perpendicular component (\perp) of the Cl-He α line is more intense than the parallel component (\parallel), resulting in the polarization degree of -0.06 , which was derived from Eq. (1) using spectral-integrated intensities I_{\parallel} and I_{\perp} . On the contrary, in Fig. 2(b), the parallel component is more intense than the perpendicular component and the polarization degree becomes $+0.10$.

Figure 3 shows dependence of polarization degrees on the tracer depth. The polarization degree critically depends on laser intensity and tracer depth. As seen in Fig. 3(a) for the low intensity, the polarization degree is initially negative close to the surface, becomes positive by a depth of about 2 μm , and ends up nearly zero for greater depth. This trend is also seen in the calculation with the 3D polarization spectroscopy model. The calculation was made as follows. First, density profile of the preplasma formed by the leakage pulse was simulated using the one-dimensional (1D) radiative hydrodynamic code ILESTA [19] to provide an initial density profile of the target. Next, electron VDFs in two-dimensional (2D) plane and 3D phase spaces were derived from a particle-in-cell (PIC) simulation. An *s*-polarized,

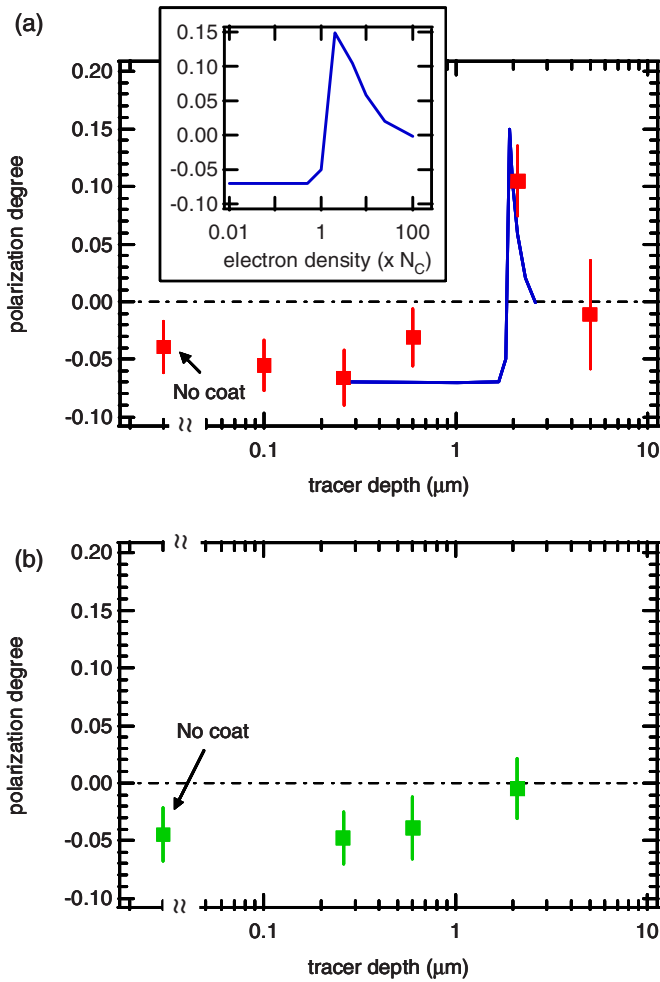


FIG. 3. (Color online) Measured polarization degree of the Cl-He α line depending on tracer depth for laser intensities of (a) 5×10^{17} W/cm 2 and (b) 4×10^{18} W/cm 2 . In (a), polarization degrees calculated by the 3D polarization spectroscopy model coupled with PIC simulations are represented with a solid line. Inset shows the same result but given as a function of electron density simulated by ILESTA.

1- μm -wavelength laser pulse of 1 ps duration irradiates the target at 7° incidence with respect to the target normal. This PIC simulation calculated temporal evolution of electron VDFs for various electron-density regions. Finally, polarization degrees were calculated by using the electron VDF and the 3D polarization spectroscopy model. In order to compare the calculation to the experiment, polarization degrees in the calculation were obtained by time integration. Calculated result is shown in Fig. 3(a) with a solid line. Inset in Fig. 3(a) shows the same result but plotted as a function of electron densities for comparison. The post-processed polarization degrees in underdense region are negative, then become positive in overdense region, and finally decrease with increase in the tracer depth, showing a good agreement with the experiment. Figure 4 shows electron spectra calculated with the PIC simulation for various electron densities. These spectra are at 350 fs after the peak of laser pulse and are integrated over a full cone angle of 20° whose center axis is laser axis. In the underdense region, electron spectra have

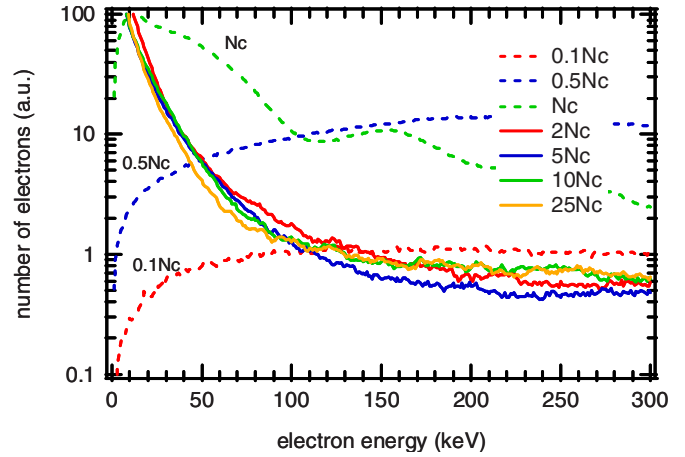


FIG. 4. (Color online) Electron spectra calculated with PIC simulations. These spectra are at 350 fs after the peak of laser pulse and are integrated over a full cone angle of 20° whose center axis is laser axis.

peaks since most of electrons in this region are highly accelerated by the laser field and quivering motion of electrons is caused. These spectra and electron VDF result in negative polarization degrees. In contrast, electron spectra in the overdense region reveal multitemperature, Maxwellian-like distributions, and electrons moving along laser axis become dominant. Therefore, polarization degrees are positive in this region. Although all slope temperatures of the distributions appear the same, PIC simulation shows that angular spread of electron VDF becomes wider with increase in the electron density. Thus, decrease of polarization degrees found in the overdense region is caused by expansion of electron VDF. Local magnetic field of several MG is generated due to the nonlinear phenomena occurring in the hot-electron flow [5]. Corresponding electron gyrofrequency becomes 10^{12} – 10^{13} Hz, comparable to the transverse diffusion collisional frequency of hot electrons in overdense region. Thus, both the magnetic and collisional effects play an important role in making the electron VDF of lower-energy component more isotropic.

On the other hand, for a high intensity, all observed polarization degrees are negative. ILESTA shows that all tracer layers exist in underdense region or around critical point. These results confirm that the measured polarization degrees are consistent with the discussion for the case of low intensity.

Anisotropy of VDF for the 2.1 μm tracer, a low-intensity shot, was evaluated from the measured polarization degree of 0.1. Consider an axially symmetric 2D VDF [16,20] where T_z and T_r are the slope temperatures of hot electrons traveling in parallel and perpendicular to the electron propagation axis z , respectively. Here, T_z was assumed to be 85 keV from the PIC simulations. Note that this temperature is close to that suggested by Wilks and Kruer [4]. Then a value of T_r of 3.3 keV was obtained from the polarization model. This corresponds to a full-angular spread of $22.4^{+5.4}_{-2.4}$, also consistent with PIC simulations and previous study [10].

IV. CONCLUSION

We have reported an x-ray polarization measurement in ultra-high-intensity laser-plasma interaction showing that x-ray polarization spectroscopy is a useful diagnostic to directly measure the electron VDF inside a plasma. Measured polarization degrees drastically changes with increase in the tracer depth. From comparison to the 3D polarization spectroscopy model, it has been shown that the spectrum and angular spread of electron VDF are strongly related to the polarization degrees. Angular spread of electron VDF in the overdense region was directly derived from the measured polarization degrees.

ACKNOWLEDGMENTS

The use to Alisé laser facility was provided though the EU access to Research Infrastructures Program “Laserlab Europe.” The authors would like to thank Y. Kimura and T. Norimatsu for their contribution to target fabrication. This work was partially supported by KAKENHI Grant No. 18340187 of Grant-in-Aid for Scientific Research (B) in Japan and grants for the Global COE Program, “Center for Electronic Devices Innovation,” from the Ministry of Education, Culture, Sports, Science, and Technology (MEXT) of Japan.

-
- [1] M. Tabak *et al.*, *Phys. Plasmas* **1**, 1626 (1994).
 [2] R. Kodama *et al.*, *Nature (London)* **418**, 933 (2002).
 [3] A. Rousse *et al.*, *Nature (London)* **410**, 65 (2001).
 [4] S. C. Wilks and W. L. Kruer, *IEEE J. Quantum Electron.* **33**, 1954 (1997), and references therein.
 [5] Y. Sentoku, K. Mima, P. Kaw, and K. Nishikawa, *Phys. Rev. Lett.* **90**, 155001 (2003).
 [6] D. Batani *et al.*, *Phys. Rev. E* **61**, 5725 (2000).
 [7] J. J. Santos *et al.*, *Phys. Plasmas* **14**, 103107 (2007).
 [8] S. N. Chen *et al.*, *Phys. Plasmas* **14**, 102701 (2007).
 [9] J. J. Santos *et al.*, *Phys. Rev. Lett.* **89**, 025001 (2002).
 [10] J. S. Green *et al.*, *Phys. Rev. Lett.* **100**, 015003 (2008).
 [11] L. O. Silva, R. A. Fonseca, J. W. Tonge, W. B. Mori, and J. M. Dawson, *Phys. Plasmas* **9**, 2458 (2002).
 [12] E. Haug, *Sol. Phys.* **71**, 77 (1981).
 [13] K. Akita, *Sol. Phys.* **86**, 101 (1983).
 [14] T. Fujimoto and A. Iwamae, *Plasma Polarization Spectroscopy* (Springer-Verlag, Berlin, 2007).
 [15] J. C. Kieffer, J. P. Matte, H. Pepin, M. Chaker, Y. Beaudoin, T. W. Johnston, C. Y. Chien, S. Coe, G. Mourou, and J. Dubau, *Phys. Rev. Lett.* **68**, 480 (1992).
 [16] Y. Inubushi *et al.*, *J. Quant. Spectrosc. Radiat. Transf.* **99**, 305 (2006); **101**, 191 (2006).
 [17] Y. Inubushi, T. Kai, T. Nakamura, S. Fujioka, H. Nishimura, and K. Mima, *Phys. Rev. E* **75**, 026401 (2007).
 [18] T. Kawamura, T. Kai, F. Koike, S. Nakazaki, Y. Inubushi, and H. Nishimura, *Phys. Rev. Lett.* **99**, 115003 (2007).
 [19] H. Takabe *et al.*, *Phys. Fluids* **31**, 2884 (1988).
 [20] Y. Inubushi, T. Kai, T. Kawamura, S. Fujioka, H. Nishimura, and K. Mima, *J. Plasma Fusion Res.* **2**, 013 (2007).